

Supporting Information

P-type molecular doping by charge transfer in halide perovskite

Julie Euvrard,^a Oki Gunawan,^b Xinjue Zhong,^c Steven P. Harvey,^d Antoine Kahn,^c David B. Mitzi^{*e}

a. Department of Mechanical Engineering and Materials Science, Duke University, Durham, North Carolina 27708, USA.

b. IBM T. J. Watson Research Center, Yorktown Heights, NY, 10598 USA.

c. Department of Electrical and Computer Engineering, Princeton University, Princeton, NJ, 08544, USA.

d. National Renewable Energy Laboratory, Golden, CO 80401, USA.

e. Department of Chemistry, Duke University, Durham, North Carolina 27708, USA.

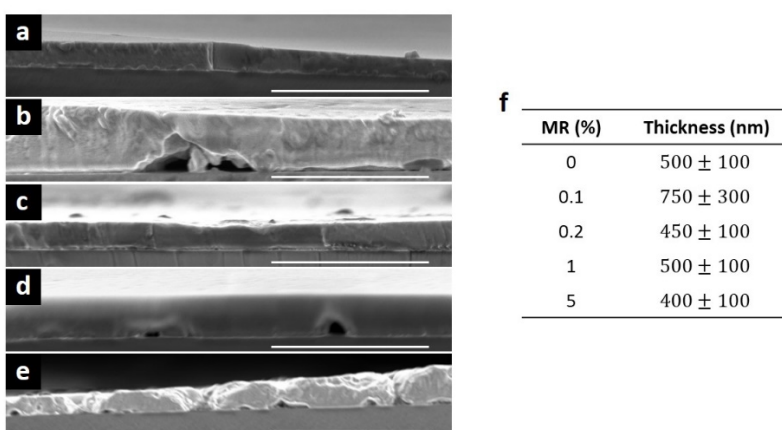


Fig. S1 Selected SEM cross-section images of MAPb_{0.5}Sn_{0.5}I₃ films with (a) 0%, (b) 0.1%, (c) 0.2%, (d) 1% and (e) 5% MR (molar ratio) F4TCNQ deposited on glass. (f) Averaged thickness of the layers over 6 to 12 different measurements along each film. The scale bar is 3 μ m.

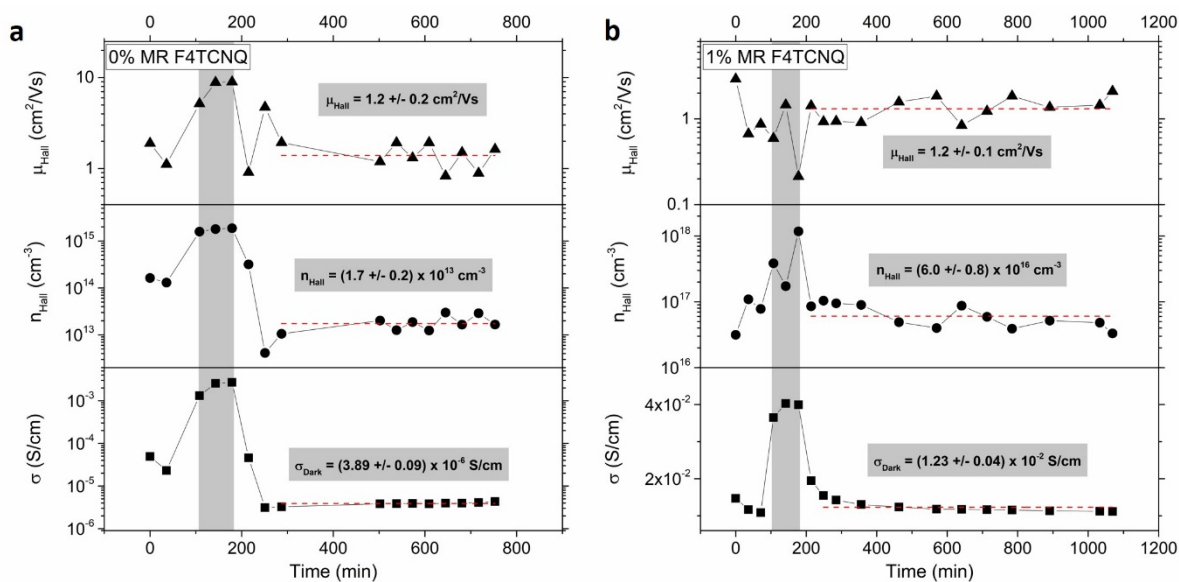


Fig. S2 Time evolution of the conductivity σ , Hall density n_{Hall} and mobility μ_{Hall} extracted in the dark and under illumination (grey region) for (a) undoped and (b) 1% MR (molar ratio) doped MAPb_{0.5}Sn_{0.5}I₃ films. Equilibrium in the dark is reached after waiting approximately one hour. Light excitation is performed with a red laser (638 nm) with a light intensity of 0.04 W/cm².

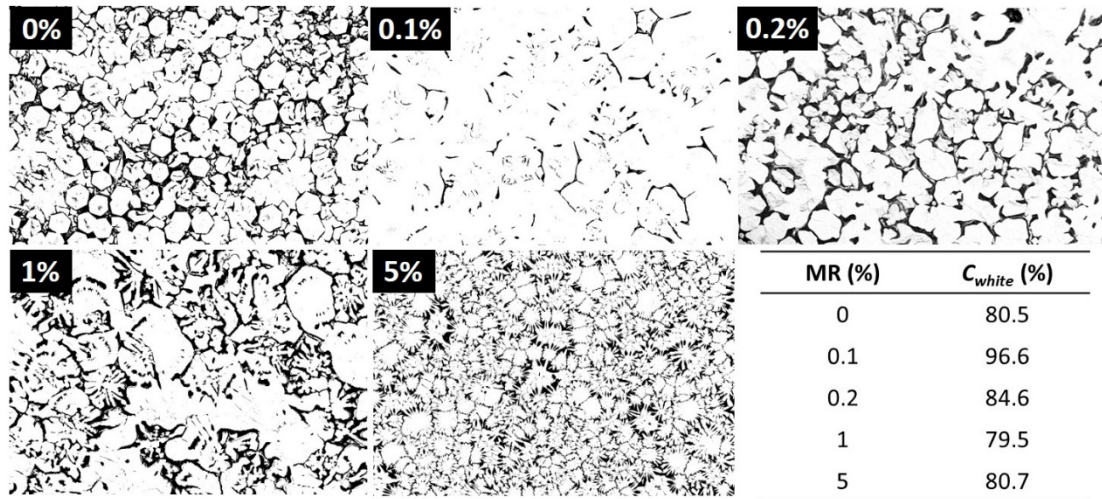


Fig. S3 SEM images transformed into black and white images for pristine 0%, 0.1%, 0.2%, 1% and 5% MR (molar ratio) F4TCNQ-doped $\text{MAPb}_{0.5}\text{Sn}_{0.5}\text{I}_3$ films. The table summarizes the proportion of white (perovskite) over total area C_{white} .

Percolation threshold

To determine if the percolation threshold is reached, we calculate the fraction of conducting (perovskite) over total area from SEM images and compare this value to the percolation threshold for an appropriate 2D system. The SEM image is transformed into a black and white image and the ratio of white over total pixels (C_{white}) is calculated using ImageJ. The C_{white} values are summarized in Figure S3.

Our perovskite layers can be considered as nominally 2D systems, as our thin film cross-section shows that the entire film thickness encompasses one single grain (see Figure S1).¹ For 2D systems, we can expect the percolation threshold to be lower than 0.625, as grains are surrounded by concave pores.^{2,3} The fractions of conducting/total area determined from SEM images are above this limit. Therefore, we can conclude that our samples should be above the percolation threshold, a statement confirmed by a conductivity significantly higher than the background glass conductivity expected if the percolation threshold is not met.

Impact of percolating network on Hall measurements

While the Hall coefficient is expected to increase as we get closer to the percolation threshold for 3D systems, it has been shown that the Hall coefficient remains constant even when close to the percolation threshold in 2D networks.^{4,5} Therefore, as long as the percolation threshold is reached, the measured Hall coefficient should correspond to the Hall coefficient in the conducting medium only. This implies that Hall mobilities should not depend on the percolating network. Nevertheless, we expect the Hall mobility to vary with grain boundary density if grain boundaries are not benign.

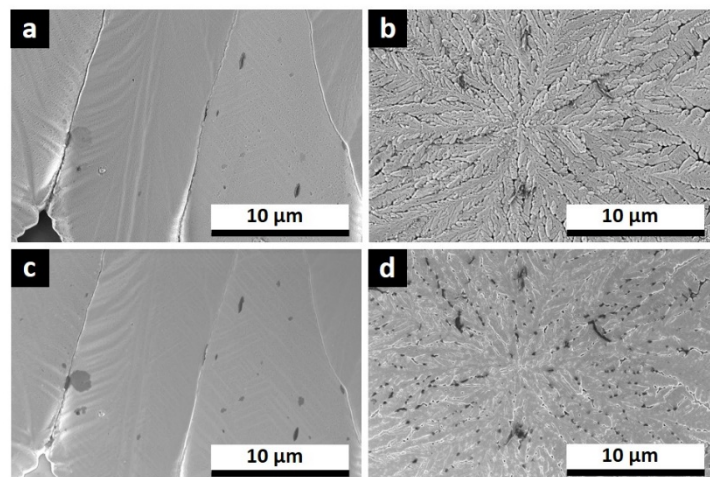


Fig. S4 SEM images of $\text{MAPb}_{0.5}\text{Sn}_{0.5}\text{I}_3$ with 1% (a ; c) and 5% (b ; d) MR (molar ratio) F4TCNQ dopant, using Trinity detectors with a 5000x magnification and collecting mostly secondary electrons (a ; b) and mostly backscattered electrons (c ; d).

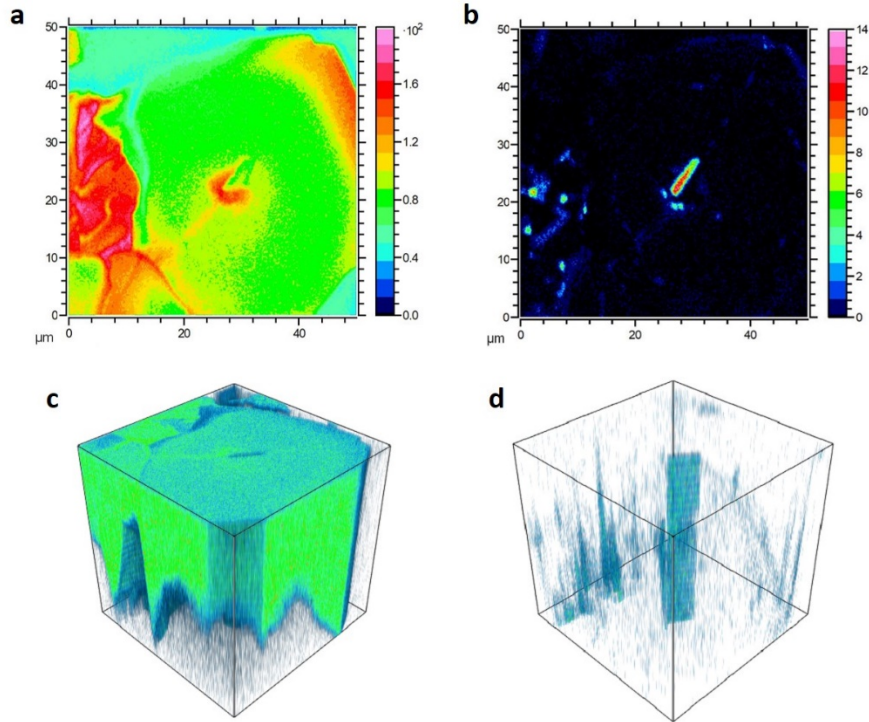


Fig. S5 TOF-SIMS 2D images of 1% MR (molar ratio) doped $\text{MAPb}_{0.5}\text{Sn}_{0.5}\text{I}_3$ (different sample from main text Fig. 3) exhibiting the total signal (a) and the F signal (b). The color scale for each image shows the intensity in counts/pixel. TOF-SIMS 3D tomography of the same sample showing the signal coming from MA (MA: methylammonium) and indicating the presence of the perovskite (c) and the F signal (d). Each 3D reconstruction is $50 \times 50 \times$ film thickness μm^3 .

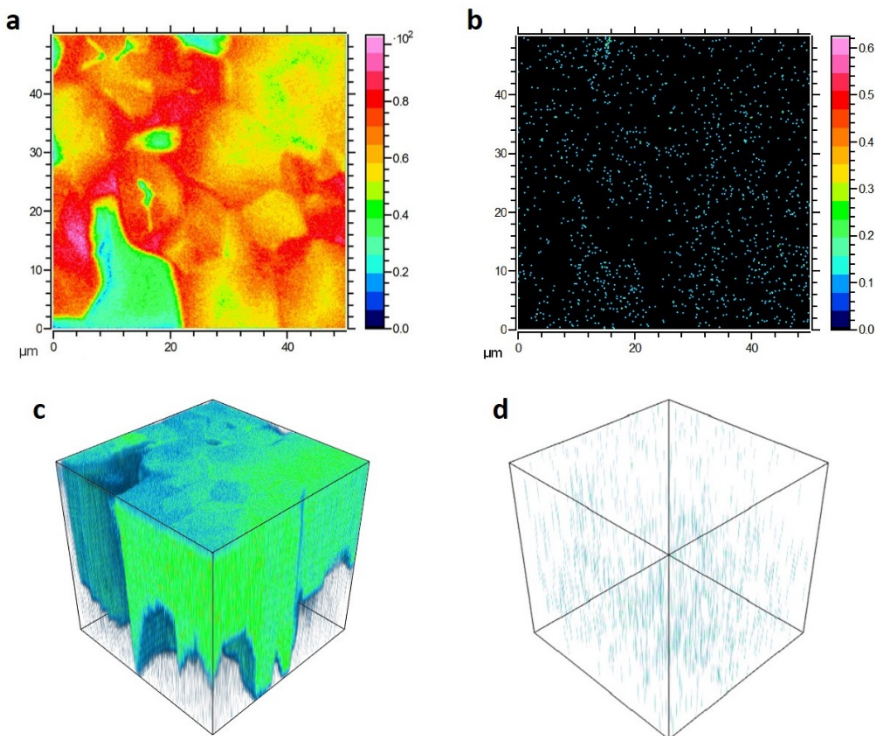


Fig. S6 TOF-SIMS 2D images of undoped $\text{MAPb}_{0.5}\text{Sn}_{0.5}\text{I}_3$ exhibiting the total signal (a) and the F signal (b). The color scale for each image shows the intensity in counts/pixel. TOF-SIMS 3D tomography of the same sample showing the signal coming from MA (MA: methylammonium) and indicating the presence of the perovskite (c) and the F signal (d). Each 3D reconstruction is $50 \times 50 \times$ film thickness μm^3 . We observe the background signal for F.

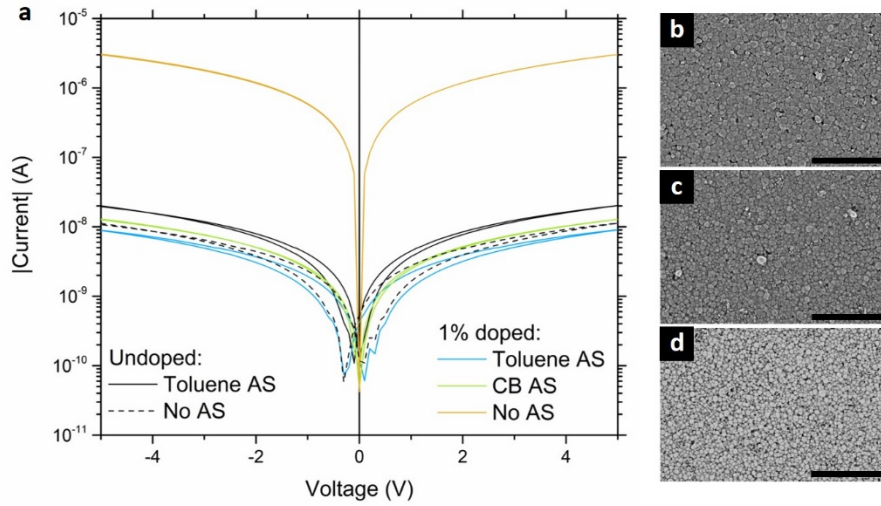


Fig. S7 (a) Current-voltage characteristics of undoped and 1% MR (molar ratio) doped $\text{MAPb}_{0.5}\text{Sn}_{0.5}\text{I}_3$ films processed under different conditions: with toluene as antisolvent (AS), with chlorobenzene (CB) as antisolvent and without antisolvent. SEM images of $\text{MAPb}_{0.5}\text{Sn}_{0.5}\text{I}_3$ films (b) undoped with toluene as antisolvent, (c) 1% MR doped with toluene as antisolvent and (d) 1% MR doped with CB as antisolvent. The scale bar is 4 μm .

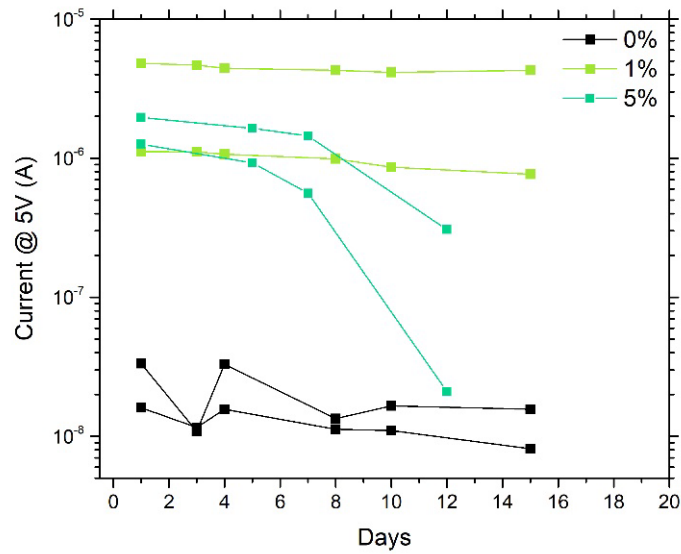


Fig. S8 Current at 5V measured over several days on encapsulated Hall bars for $\text{MAPb}_{0.5}\text{Sn}_{0.5}\text{I}_3$ films with 0%, 1% and 5% MR (molar ratio) dopant concentration.

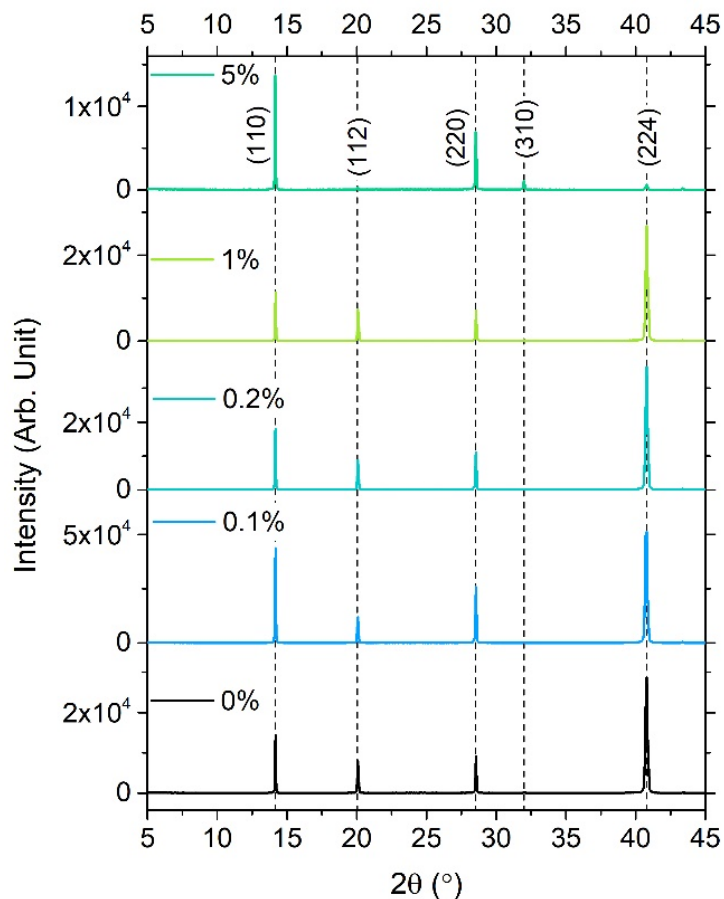


Fig. S9 XRD patterns of $\text{MAPb}_{0.5}\text{Sn}_{0.5}\text{I}_3$ films with 0%, 0.1%, 0.2%, 1% and 5% MR (molar ratio) F4TCNQ. The Miller indices of the major peaks and associated with the tetragonal $I4/mcm$ space group structure are indicated.

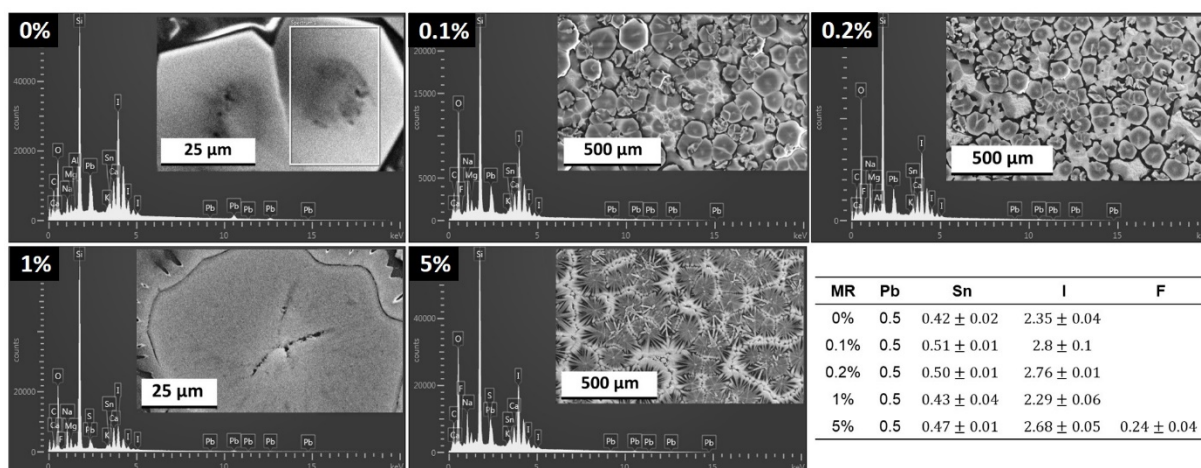


Fig. S10 EDX spectra obtained on $\text{MAPb}_{0.5}\text{Sn}_{0.5}\text{I}_3$ films with 0%, 0.1%, 0.2%, 1% and 5% F4TCNQ. The measurements are performed on three different spots and the average stoichiometry for Sn, I and F with respect to Pb are summarized in the table. We note that for 5% MR (molar ratio) F4TCNQ, we would expect a value of 0.2 for F, close to the value obtained. Nevertheless, the signal is weak for F in EDS spectra and it is difficult to quantify F content reliably.

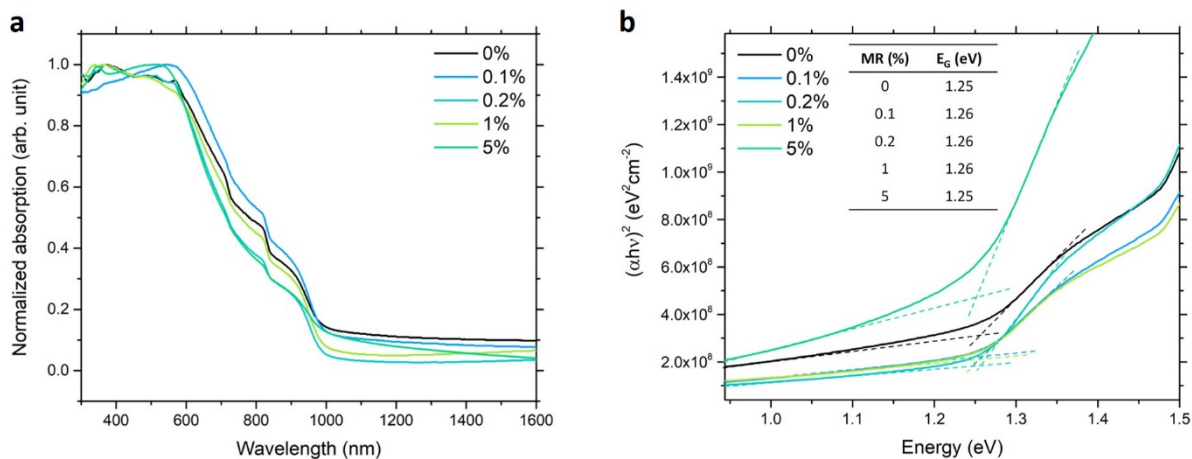


Fig. S11 Normalized absorption (a) and Tauc plot for direct bandgap (b) for $\text{MAPb}_{0.5}\text{Sn}_{0.5}\text{I}_3$ films with 0%, 0.1%, 0.2%, 1% and 5% MR (molar ratio) F4TCNQ. The inset table in b) summarizes the bandgap (E_g) extracted for each sample.

Table S1 Summary of the WF values obtained for undoped and 1% MR (molar ratio) doped $\text{MAPb}_{0.5}\text{Sn}_{0.5}\text{I}_3$ using UPS and KP-CPD measurements. Highly ordered pyrolytic graphite (HOPG) is used as reference to calibrate the WF of the Kelvin probe tip.

Samples	WF_{UPS} (eV)	WF_{KP} (eV)
Undoped	4.51	4.48
1% doped	4.73	4.85

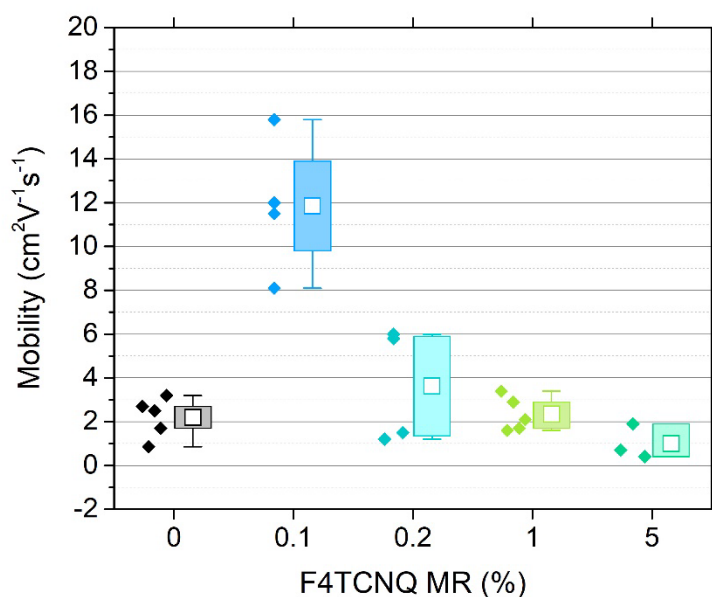


Fig. S12 Hole mobility of $\text{MAPb}_{0.5}\text{Sn}_{0.5}\text{I}_3$ films for different F4TCNQ concentration in molar ratio (MR) obtained from AC Hall effect measurements. Several samples have been measured for each dopant concentration and the box charts indicate the maximum and minimum values (whiskers), the upper quartile and lower quartile (box) and the mean value (empty square).

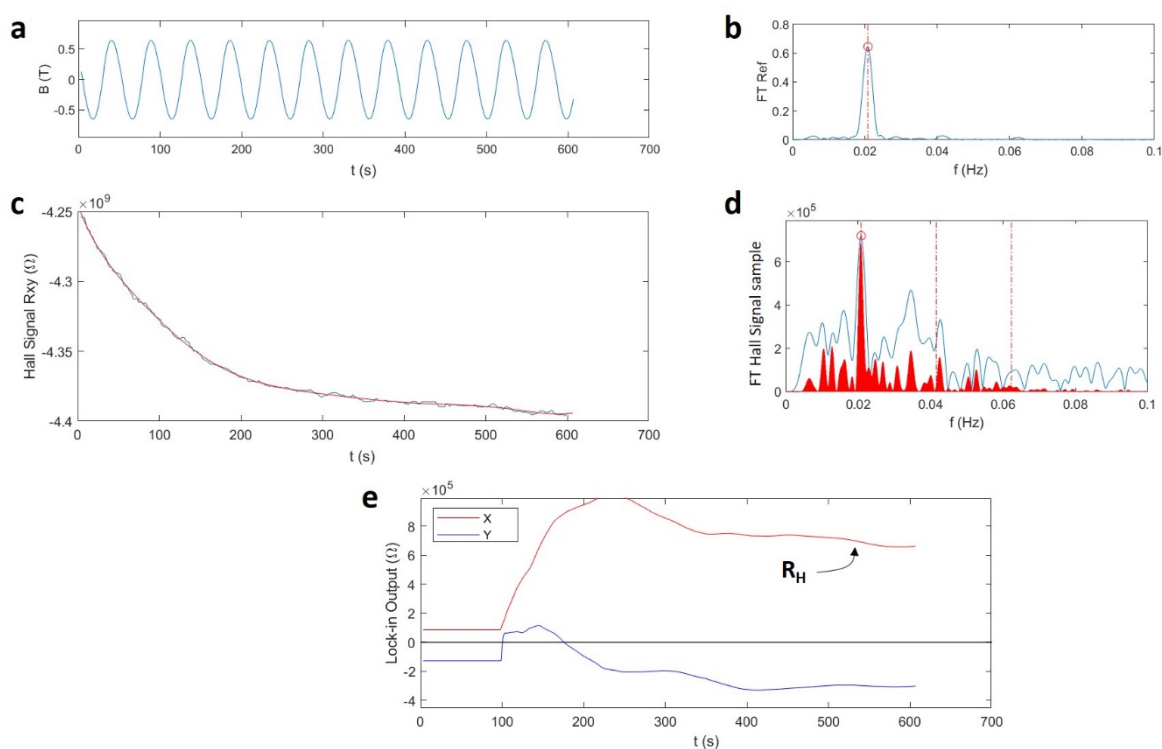


Fig. S13 Hall signal extraction on undoped $\text{MAPb}_{0.5}\text{Sn}_{0.5}\text{I}_3$ using a PDL setup: a) Magnetic field B traces as the reference signal, and b) Fourier transform of the reference signal B . c) Transverse Hall signal R_{xy} and d) Fourier transform of R_{xy} . The dashed dotted lines correspond to the second and third harmonics of the AC signal B . The red filled region is the power spectral density (PSD) and the curve is the Fourier spectra of the signal. The former accentuates the periodic signal content as shown in the fundamental first harmonic component of the signal. e) Lock-in detection of the in-phase X (Hall signal) and out-of-phase Y signals over time where the Hall resistance R_H is extracted. A lock-in time constant of 100s is used in this example. The single harmonic ac magnetic field along with lock-in detection allow the extraction of an R_H value $\sim 10^5 \Omega$ with a background resistance of $\sim 10^9 \Omega$.

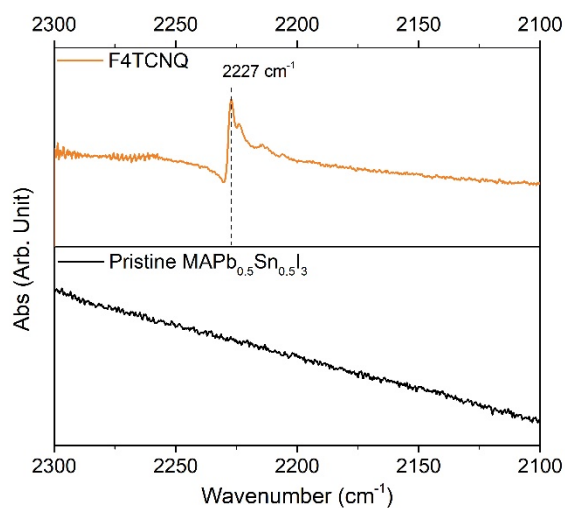


Fig. S14 FTIR absorption spectra for pristine $\text{MAPb}_{0.5}\text{Sn}_{0.5}\text{I}_3$ and pure F4TCNQ deposited from CB solution on KBr substrates.

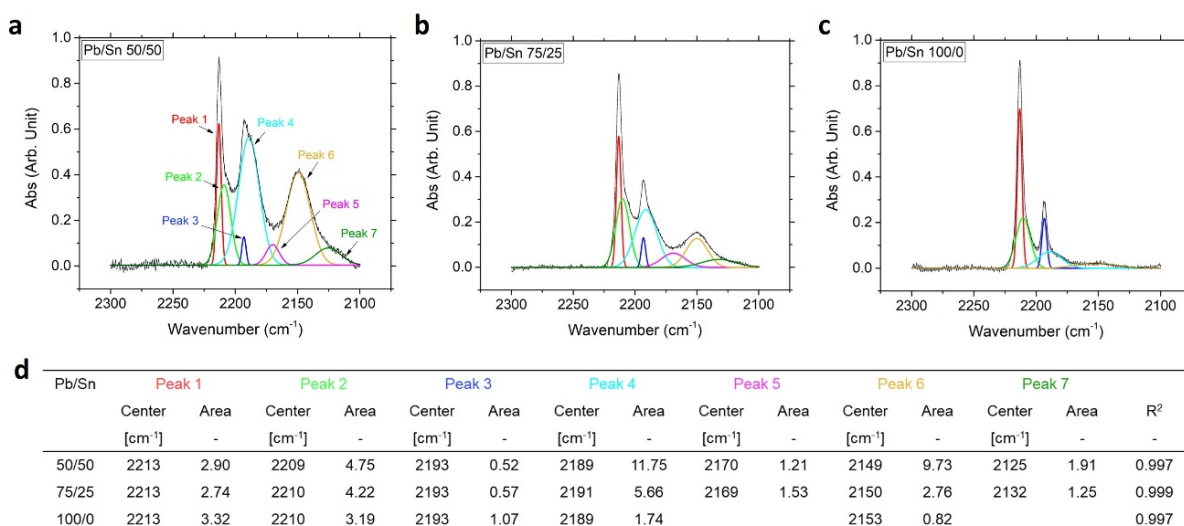


Fig. S15 Multiple Gaussian peak fitting performed on the FTIR spectra of MAPb_{1-x}Sn_xI₃ with Pb/Sn ratio of 50/50 ($x=0.5$) (a), 75/25 ($x=0.25$) (b) and 100/0 ($x=0$) (c) doped with 5% MR (molar ratio) F4TCNQ. The center and area of each peak is given in the table (d).

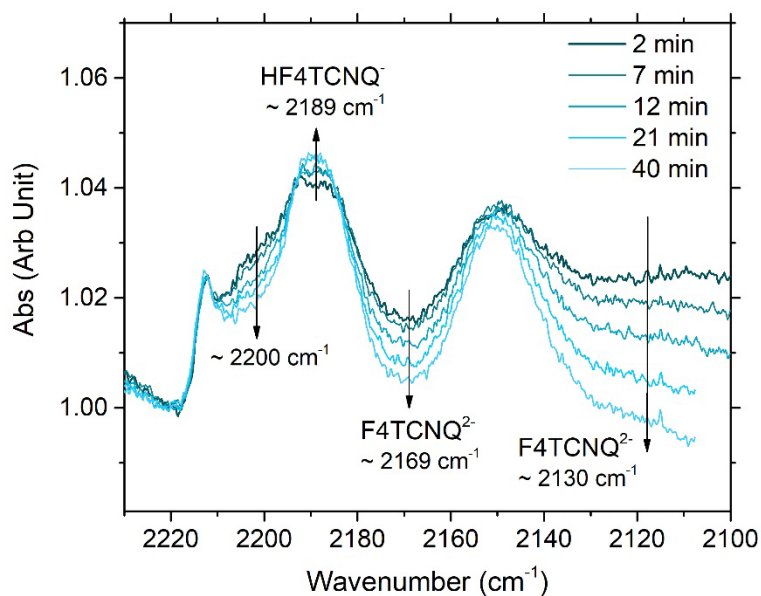


Fig. S16 FTIR absorption spectra for 5% MR (molar ratio) doped MAPb_{0.5}Sn_{0.5}I₃ over time. The first measurement (2 min) is performed 2 min after opening the sealed bag containing the sample (sealed in nitrogen environment). Each scan takes about 4 min to complete. The spectra are normalized at 2220 cm⁻¹. It is important to note that the wavenumber chosen for normalization influences the observation of peak intensity evolution. Nevertheless, it is clear the F4TCNQ²⁻ contribution is decreasing over time.

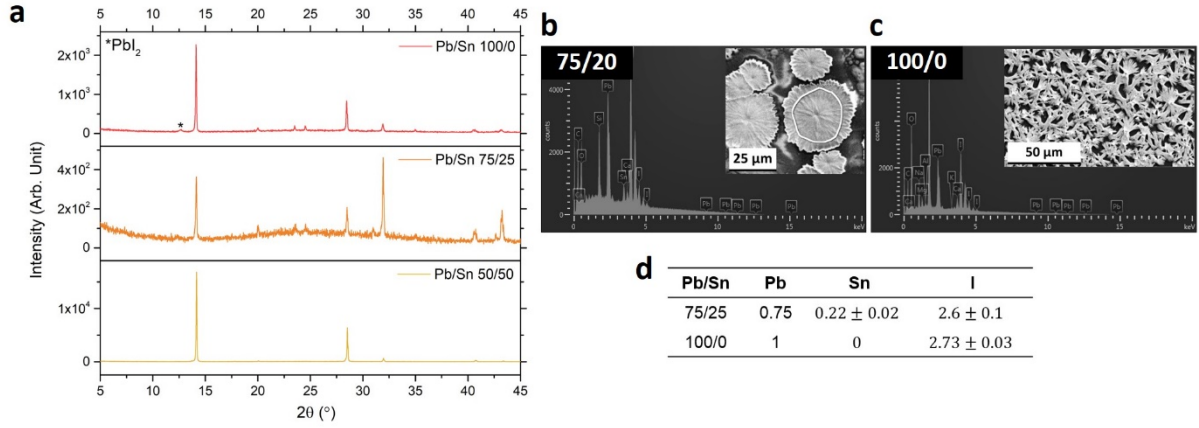


Fig. S17 XRD patterns of 5% MR (molar ratio) doped $\text{MAPb}_{1-x}\text{Sn}_x\text{I}_3$ with Pb/Sn ratio of 50/50 ($x=0.5$), 75/25 ($x=0.25$) and 100/0 ($x=0$) (a). EDX spectra obtained on $\text{MAPb}_{0.75}\text{Sn}_{0.25}\text{I}_3$ (b) and MAPbI_3 (c). The measurements are performed on three different spots and the average stoichiometry for Sn and I with respect to Pb are summarized in the table (d).

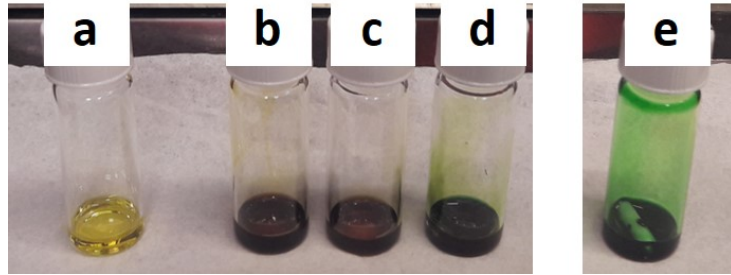


Fig. S18 Picture of the $\text{MAPb}_x\text{Sn}_{1-x}\text{I}_3$ precursor solutions taken immediately after filtration: undoped Pb/Sn 50/50 (a), 5% MR (molar ratio) doped Pb/Sn 50/50 (b), 5% doped Pb/Sn 75/25 (c) and 5% doped Pb/Sn 100/0 (d). Picture of MAI:F4TCNQ solution in DMF:DMSO (80:20 in volume) (e). Of note, the color does not change significantly with time over a period of a few weeks when stored in nitrogen.

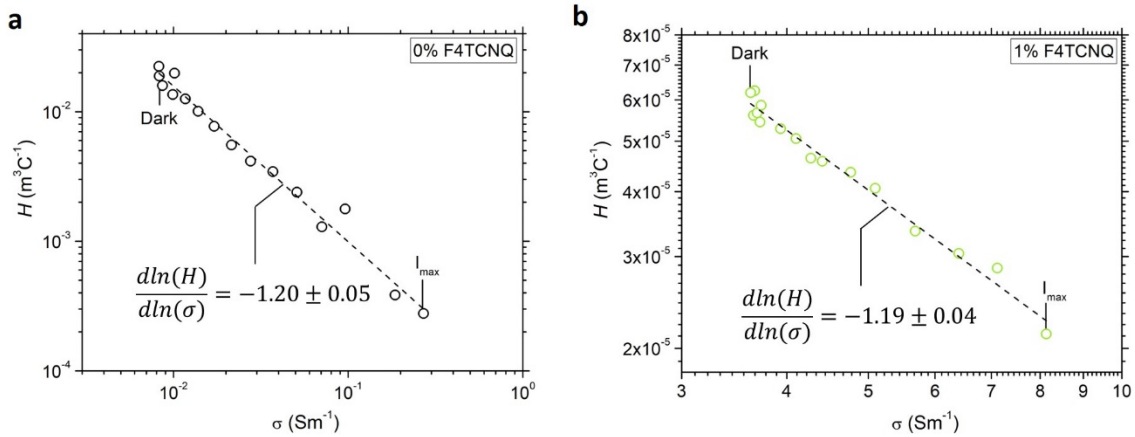


Fig. S19 Carrier-resolved photo Hall H - σ plot with an excitation wavelength of 638 nm for undoped (a) and 1% MR (molar ratio) doped (b) $\text{MAPb}_{0.5}\text{Sn}_{0.5}\text{I}_3$. A maximum light intensity $I_{\text{max}} = 30 \text{ mWcm}^{-2}$ is used.

CRPH analysis with $\Delta p \geq \Delta n$

In the case where $\Delta p \neq \Delta n$ (Δp and Δn being the photogenerated hole and electron densities), the conductivity for a p-type semiconductor under illumination should be written as:

$$\sigma = q(\mu_p(p_0 + \Delta p) + \mu_n \Delta n), \quad (\text{S1})$$

with q the elementary charge, μ_p and μ_n the hole and electron mobilities and p_0 the background carrier density. Δp and Δn are related to the hole τ_p and electron τ_n recombination lifetimes (which are different when $\Delta p \neq \Delta n$) according to:

$$\frac{\Delta n}{\tau_n} = \frac{\Delta p}{\tau_p}. \quad (S2)$$

Taking into account the parameter $\beta = \frac{\mu_n}{\mu_p}$, equation (S1) can be written:

$$\sigma = q\mu_p \left(p_0 + \Delta p \left(1 + \beta \frac{\tau_n}{\tau_p} \right) \right). \quad (S3)$$

From equation (S3), we can deduce Δp for a p-type material when $\Delta p \neq \Delta n$

$$\Delta p = \frac{\sigma(1 - \beta) - qp_0\Delta\mu}{q \left(1 + \beta \frac{\tau_n}{\tau_p} \right) \Delta\mu}. \quad (S4)$$

Note that $\Delta\mu = \mu_p - \mu_n$. In the standard CRPH analysis, considering $\Delta p = \Delta n$, Δp_{CRPH} is given by:

$$\Delta p_{CRPH} = \frac{\sigma(1 - \beta^2) - qp_0\Delta\mu(1 + \beta)}{q\Delta\mu(1 + \beta)^2}. \quad (S5)$$

Therefore, if we multiply equation (S4) by $\frac{1+\beta}{1+\beta}$, we can write:

$$\Delta p(\Delta p \neq \Delta n) = \Delta p_{CRPH} \frac{(1 + \beta)}{\left(1 + \beta \frac{\tau_n}{\tau_p} \right)}. \quad (S6)$$

Of note, if $\Delta p = \Delta n$, we obtain $\Delta p = \Delta p_{CRPH}$ from equation (S6), as expected. Moreover, if $\beta \rightarrow 0$, we also obtain $\Delta p = \Delta p_{CRPH}$ (even if $\Delta p \neq \Delta n$). Therefore, when there is a large imbalance of mobility, we obtain the lifetime of the majority type carriers, here holes. For a given value of β , we find that:

$$\Delta p(\Delta p \neq \Delta n) \xrightarrow[\frac{\tau_n}{\tau_p} \rightarrow 0]{} \Delta p_{CRPH} \times (1 + \beta), \text{ and} \quad (S7)$$

$$\Delta p(\Delta p \neq \Delta n) \xrightarrow[\frac{\tau_n}{\tau_p} \rightarrow 1]{} \Delta p_{CRPH} \quad (S8)$$

From equations (S7) and (S8), we know that Δp is bonded between $\Delta p \left(\frac{\tau_n}{\tau_p} = 1 \right)$ and $\Delta p \left(\frac{\tau_n}{\tau_p} = 0 \right)$, if the function Δp (equation (S6)) monotonously decreases with $\frac{\tau_n}{\tau_p}$ between 0 and 1. This condition is verified with the determination of $\frac{d\Delta p}{d\frac{\tau_n}{\tau_p}}$ for $0 \leq \frac{\tau_n}{\tau_p} \leq 1$:

$$\frac{d\Delta p}{d\frac{\tau_n}{\tau_p}} = - \frac{\Delta p_{CRPH}(1 + \beta)\beta}{\left(1 + \beta \frac{\tau_n}{\tau_p} \right)^2}. \quad (S9)$$

Since $\beta \geq 0$, we can show that $\frac{d\Delta p}{d\frac{\tau_n}{\tau_p}} \leq 0$ and, therefore, monotonously decreases with $\frac{\tau_n}{\tau_p}$. Finally, we can write that, for $\Delta p \geq \Delta n$,

$$\Delta p_{CRPH} \leq \Delta p \leq \Delta p_{CRPH}(1 + \beta). \quad (S10)$$

Since $\tau = \Delta p/G$, we can write, for $\Delta p \geq \Delta n$,

$$\tau_{CRPH} \leq \tau_p \leq \tau_{CRPH}(1 + \beta), \quad (S11)$$

where τ_{CRPH} is the carrier recombination lifetime calculated with the standard CRPH model considering $\Delta p = \Delta n$, and τ_p is the true hole recombination lifetime for $\Delta p \geq \Delta n$.

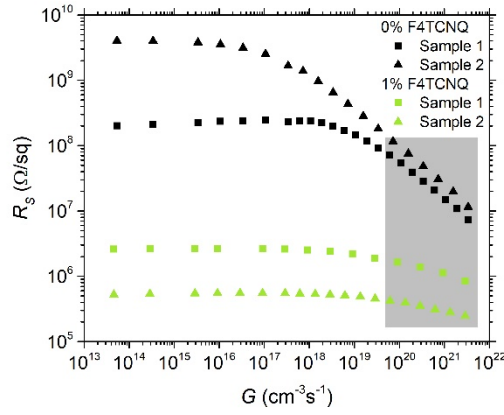


Fig. S20 Sheet resistance R_s as a function of generation rate G for two undoped and two 1% MR (molar ratio) doped $\text{MAPb}_{0.5}\text{Sn}_{0.5}\text{I}_3$ samples. The grey area highlights the resistance decrease upon photocarrier generation.

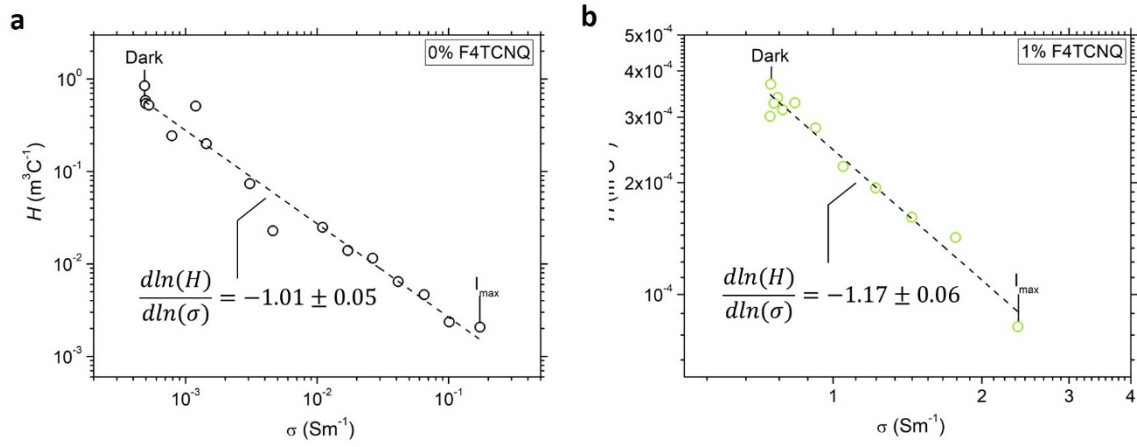


Figure S21. Carrier-resolved photo Hall H - σ plot for a second sample of undoped (a) and 1% MR (molar ratio) doped (b) $\text{MAPb}_{0.5}\text{Sn}_{0.5}\text{I}_3$. A maximum light intensity $I_{max} = 30 \text{ mWcm}^{-2}$ is used.

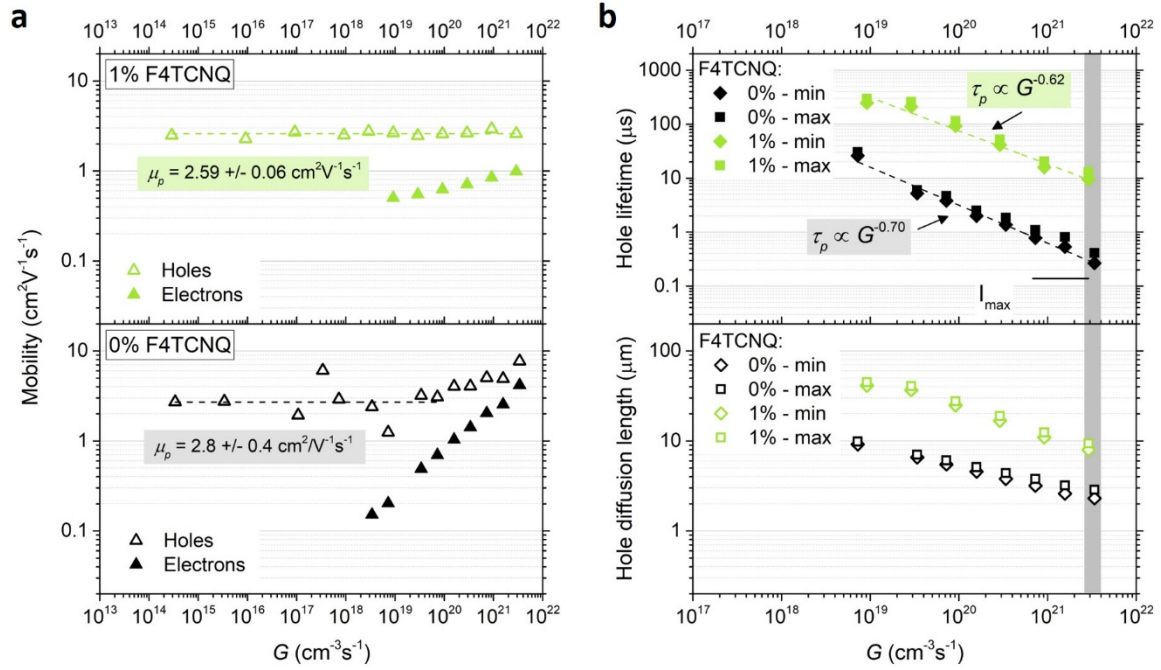


Figure S22. (a) Hole μ_p and electron μ_n mobilities as a function of generation rate G extracted from CRPH measurements for a second sample of 0% and 1% MR (molar ratio) doped $\text{MAPb}_{0.5}\text{Sn}_{0.5}\text{I}_3$. (b) Hole lifetime τ_p and diffusion length $L_{d,p}$ for 0% and 1% doped $\text{MAPb}_{0.5}\text{Sn}_{0.5}\text{I}_3$. A linear fit at high light intensity provides the power law $\tau_p \propto G^{-1}$. The grey area highlights the data points obtained at the highest light intensity $I_{\text{max}} = 30 \text{ mWcm}^{-2}$ (approximately a third of one sun intensity).

References

- 1 Y.-B. Yi, C.-W. Wang and A. M. Sastry, *J. Electrochem. Soc.*, 2004, **151**, A1292.
- 2 J. Lin, W. Zhang, H. Chen, R. Zhang and L. Liu, *Int. J. Heat Mass Transf.*, 2019, **138**, 1333–1345.
- 3 D. R. Baker, G. Paul, S. Sreenivasan and H. E. Stanley, *Phys. Rev. E - Stat. Physics, Plasmas, Fluids, Relat. Interdiscip. Top.*, 2002, **66**, 5.
- 4 J. W. Orton and M. J. Powell, *Reports Prog. Phys.*, 1980, **43**, 1263–1307.
- 5 C. J. Adkins, *J. Phys. C Solid State Phys.*, 1979, **12**, 3389–3393.